NANO MICRO
small

Postfach 10 11 61
69451 Weinheim
Germany
Courier services:
Boschstraße 12
69469 Weinheim
Germany
Tel.: (+49) 6201 606 235
Fax: (+49) 6201 606 500
E-mail: small@wiley.com

WILEY-VCH

Dear Author,

Please correct your galley proofs carefully and return them no more than four days after the page proofs have been received.

Please limit corrections to errors already in the text; cost incurred for any further changes or additions will be charged to the author, unless such changes have been agreed upon by the editor.

The editors reserve the right to publish your article without your corrections if the proofs do not arrive in time.

Note that the author is liable for damages arising from incorrect statements, including misprints.

Please note any queries that require your attention. These are indicated with a Q in the PDF and a question at the end of the document.

Reprints may be ordered by filling out the accompanying form.

Return the reprint order form by fax or by e-mail with the corrected proofs, to Wiley-VCH : small@wiley.com

To avoid commonly occurring errors, **please ensure that the following important items are correct** in your proofs (please note that once your article is published online, no further corrections can be made):

- **Names** of all authors present and spelled correctly
- **Titles** of authors correct (Prof. or Dr. only: please note, Prof. Dr. is not used in the journals)
- **Addresses** and **postcodes** correct
- **E-mail address** of corresponding author correct (current email address)
- **Funding bodies** included and grant numbers accurate
- **Title** of article OK
- All **figures** included
- **Equations** correct (symbols and sub/superscripts)

Corrections should be made directly in the PDF file using the PDF annotation tools. If you have questions about this, please contact the editorial office. The corrected PDF and any accompanying files should be uploaded to the journal's Editorial Manager site.

Author Query Form

WILEY

Journal SMLL

Article smll202003290

Dear Author,

During the copyediting of your manuscript the following queries arose.

Please refer to the query reference callout numbers in the page proofs and respond to each by marking the necessary comments using the PDF annotation tools.

Please remember illegible or unclear comments and corrections may delay publication.

Many thanks for your assistance.

Query No.	Description	Remarks
Q-OO	Open access publication of this work is possible via Wiley OnlineOpen. Information about this is available at: https://authorservices.wiley.com/author-resources/Journal-Authors/licensing-open-access/open-access/onlineopen.html. The cost of publishing your manuscript OnlineOpen may be covered by one of Wiley's national agreements. To find out more, visit https://authorservices.wiley.com/author-resources/Journal-Authors/open-access/affiliation-policies-payments/index.html. Note that eligibility for fee coverage is determined by the affiliation of the primary corresponding author designated at submission. Please log in to your Wiley Author Services account at https://authorservices.wiley.com/ and confirm your affiliation to see if you are eligible. Instructions for placing an OnlineOpen order can be found at: https://authorservices.wiley.com/author-resources/Journal-Authors/open-access/how-to-order-onlineopen.html. To publish your article open access, please complete the order process before completing your proof corrections.	
Q1	Please confirm that forenames/given names (blue) and surnames/family names (vermilion) have been identified correctly.	
Q2	Please provide the highest academic title (either Dr. or Prof.) for all authors, where applicable.	
Q3	Both 'Aix Marseille Univ' and 'Aix-Marseille Univ' were given in the affiliations. For consistency 'Aix-Marseille Université' is followed. Please check for correctness.	
Q4	Please define all acronyms at their first appearance in the abstract, text and table of contents, respectively. Only expanded forms are allowed if the elements are cited only once in the article.	

Please confirm that Funding Information has been identified correctly.

Please confirm that the funding sponsor list below was correctly extracted from your article: that it includes all funders and that the text has been matched to the correct FundRef Registry organization names. If a name was not found in the FundRef registry, it may not be the canonical name form, it may be a program name rather than an organization name, or it may be an organization not yet included in FundRef Registry. If you know of another name form or a parent organization name for a "not found" item on this list below, please share that information.

FundRef Name	FundRef Organization Name
Michel Skandalovski	
CERIMED	
Aix-Marseille University	Aix
Samy Vigier	
Faculty of Pharmacy	
Aix-Marseille University	Aix
Ligue Nationale Contre le Cancer	
China Scholarship Council	China Scholarship Council
Italian Association	
Cancer Research	

FundRef Name	FundRef Organization Name
EURONANOMED European Research	
National Natural Science Foundation of China	
Ecole Doctorale 62 Sciences	National Natural Science Foundation of China
Aix-Marseille Université	
Cancer Nanomedicine	Aix
Bench to the Bedside	
European Cooperation in Science and Technology	European Cooperation in Science and Technology

L. Ding, Z. Lyu, B. Louis, A. Tintaru, E. Laurini, D. Marson, M. Zhang, W. Shao, Y. Jiang, A. Bouhlel, L. Balasse, P. Garrigue, E. Mas, S. Giorgio, J. Iovanna, Y. Huang, S. Pricl, B. Guillet, L. Peng*..... 2003290

Surface Charge of Supramolecular Nanosystems for In Vivo Biodistribution: A Microspect/CT Imaging Study

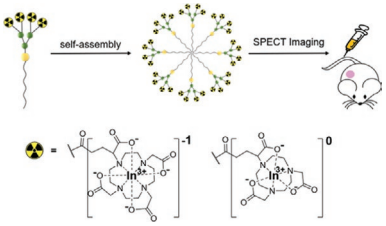

Replacing the DOTA cage with the NOTA scaffold to chelate the radionuclide In^{3+}, the corresponding dendrimer nanosystem completely reverses the zeta-potential from negative to positive, generates a highly favorable biodistribution profile with a drastically reduced uptake in liver, and exhibits significantly improved tumor imaging.

NANO · MICRO small
www.small-journal.com

Surface Charge of Supramolecular Nanosystems for In Vivo Biodistribution: A Microspect/CT Imaging Study

Ling Ding, Zhenbin Lyu, Beatrice Louis, Aura Tintaru, Erik Laurini, Domenico Marson, Mengjie Zhang, Wanxuan Shao, Yifan Jiang, Ahlem Bouhlel, Laure Balasse, Philippe Garrigue, Eric Mas, Suzanne Giorgio, Juan Iovanna, Yuanyu Huang, Sabrina Pricl, Benjamin Guillet, and Ling Peng*

Bioimaging has revolutionized medicine by providing accurate information for disease diagnosis and treatment. Nanotechnology-based bioimaging is expected to further improve imaging sensitivity and specificity. In this context, supramolecular nanosystems based on self-assembly of amphiphilic dendrimers for single photon emission computed tomography (SPECT) bioimaging are developed. These dendrimers bear multiple In^{3+} radionuclides at their terminals as SPECT reporters. By replacing the macrocyclic DOTA cage with the smaller NOTA scaffold as the In^{3+} chelator, the corresponding dendrimer exhibits neutral In^{3+}-complex terminals in place of negatively charged In^{3+}-complex terminals. This negative-to-neutral surface charge alteration completely reverses the zeta-potential of the nanosystems from negative to positive. As a consequence, the resulting SPECT nanoprobe generates a highly sought-after biodistribution profile accompanied by a drastically reduced uptake in liver, leading to significantly improved tumor imaging. This finding contrasts with current literature reporting that positively charged nanoparticles have preferential accumulation in the liver. As such, this study provides new perspectives for improving the biodistribution of positively charged nanosystems for biomedical applications.

1. Introduction

Molecular imaging has revolutionized cancer management by providing precise information relating to tumor detection, grading, staging, and diagnosis, as well as monitoring treatment response and efficacy for personalized medicine.[1,2] Nevertheless, there is high demand for further improvements in terms of sensitivity, specificity, and spatial resolution. Nanotechnology is expected to overcome these limitations by further improving imaging sensitivity and specificity via the so-called "enhanced permeability and retention (EPR)" effect, also termed passive tumor targeting.[3–5] EPR allows nanosized macromolecules or particles to preferentially accumulate in tumor tissue because of the leaky vasculature and disabled lymphatic system characterizing the tumor

L. Ding, Z. Lyu, Y. Jiang, S. Giorgio, L. Peng
Aix-Marseille Université
CNRS
Centre Interdisciplinaire de Nanoscience de Marseille (CINaM), UMR 7325
Equipe Labellisée Ligue Contre le Cancer
Marseille, France
E-mail: ling.peng@univ-amu.fr

L. Ding
Aix-Marseille Université
CNRS
Centre de Résonance Magnétique Biologique et Médicale (CRMBM), UMR 7339
Marseille, France

Z. Lyu, A. Tintaru
Aix-Marseille Université
CNRS
Institut de Chimie Radicalaire (ICR)
Marseille, France

B. Louis, A. Bouhlel, L. Balasse, P. Garrigue, B. Guillet
Aix-Marseille Université
INSERM
INRAE, C2VN
Marseille, France

The ORCID identification number(s) for the author(s) of this article can be found under https://doi.org/10.1002/smll.202003290.

DOI: 10.1002/smll.202003290

B. Louis, A. Bouhlel, L. Balasse, P. Garrigue, B. Guillet
Aix-Marseille Université
CNRS
CERIMED
Marseille, France

E. Laurini, D. Marson, S. Pricl
Molecular Biology and Nanotechnology Laboratory (MolBNL@UniTS)
DEA
University of Trieste
Trieste, Italy

M. Zhang, W. Shao, Y. Huang
School of Life Science
Advanced Research Institute of Multidisciplinary Science
Institute of Engineering Medicine
Key Laboratory of Molecular Medicine and Biotherapy
Beijing Institute of Technology
Beijing, China

E. Mas, J. Iovanna
Aix-Marseille Université
INSERM
CRCM
Marseille, France

S. Pricl
Department of General Biophysics
Faculty of Biology and Environmental Protection
University of Lodz
Lodz, Poland

microenvironment.[6] As a result, the local concentration of imaging agents in tumor lesions can be significantly increased, leading to better imaging outcomes. Moreover, nanosystems can carry multiple or hundreds of imaging reporters, which can significantly enhance the contrast signal for more accurate imaging and diagnosis. Consequently, different nanosystems have been explored and studied for tumor imaging.[3–5]

Dendrimer nanosystems are of particular interest for the delivery of imaging agents because of the unique dendritic structure and multivalent cooperativity confined within the nanoscale dimension.[7–12] We have recently established small amphiphilic dendrimers that are able to self-assemble into supramolecular nanosystems for effective tumor imaging using positron emission tomography (PET) and single photon emission computed tomography (SPECT) (**Figure 1**).[13,14] Both PET and SPECT are radio-imaging techniques that have a high sensitivity yet unlimited tissue penetration, and are able to visualize functional information quantitatively.[15,16] Notably, SPECT is the most prevalent clinical imaging modality, accounting for > 75% of all nuclear imaging procedures.[17] Thus, we have focused our recent efforts on optimizing our supramolecular dendrimer systems for SPECT imaging.

We previously developed an amphiphilic dendrimer **In-1** composed of a long hydrophobic alkyl chain and a hydrophilic poly(amidoamine) dendron bearing the SPECT radionuclide ^{111}In(III) complexed with the macrocycle DOTA (1,4,7,10-tetraazacyclododecane-1,4,7,10-tetraacetic acid) ring in the chelator DOTAGA (1,4,7,10-tetraazacyclododececane-1-(glutaric acid)-4,7,10-triacetic acid) at the terminals (**In-1** in Figure 1).[14] By virtue of its amphiphilic nature, **In-1** self-assembled into small and stable supramolecular nanomicelles for effective SPECT imaging of tumors based on the favorable combination of EPR-based passive tumor targeting and the dendrimeric structure bearing multivalent SPECT reporters. Nevertheless, **In-1** also displayed high liver retention, which represents a severe limitation for its future clinical translation.

It is well known that different chelators can significantly impact the biodistribution of radiotracers based on their size, charge, geometry, and lipophilicity when complexed with radionuclide metal ions.[18–20] As the macrocycle DOTA ring in the DOTAGA chelator forms a negatively charged complex with In^{3+}, we suspected that, despite the small nanosize of the corresponding **In-1** nanomicelle, the overall surface charge of the **In-1** nanoparticle might cause the high liver uptake and retention. Thus, we hypothesized that suppressing the negative surface charge of the dendrimer could limit this unfavorable liver retention. Accordingly, we replaced the macrocyclic DOTA cage with the NOTA (1,4,7-triazacyclononane-1,4,7-triacetic acid) scaffold by conjugating the chelator NODAGA (1,4,7-triazacyclononane,1-glutaric acid-4,7-acetic acid) at the dendrimer terminals, because the NOTA ring can form a neutral complex when chelating the trivalent metal ion In^{3+} (**In-2** in Figure 1).[21] Also, the macrocycle NOTA scaffold is smaller than the DOTA cage, and hence generates more stable complexes with small metal ions, such as Ga^{3+}, In^{3+}, and Cu^{2+}.[22] It should be noted that here we use DOTA and NOTA cages or rings as macrocyclic scaffolds for complexing with metal ions, rather than as the specific chelators in this work. Their corresponding chelators used in this work, DOTAGA and NODAGA, are, respectively, DOTA and NOTA-derivatives, often used for convenient conjugation with other chemical entities to present DOTA and NOTA scaffolds, thus maintaining the full denticity of DOTA and NOTA when chelating with metal ions.

Indeed, changing the DOTA cage to the NOTA ring at the amphiphilic dendrimer terminals had a profound impact on the surface charge of the resulting dendrimer, completely reversing the zeta potential from negative to positive when complexing with the trivalent metal ion In^{3+}. As a consequence of this alteration, the radioactive In^{3+}-labeled imaging nanoprobe **In-2** led to a highly favorable biodistribution with drastically reduced uptake in liver, generating significantly improved tumor imaging. Although current literature reports

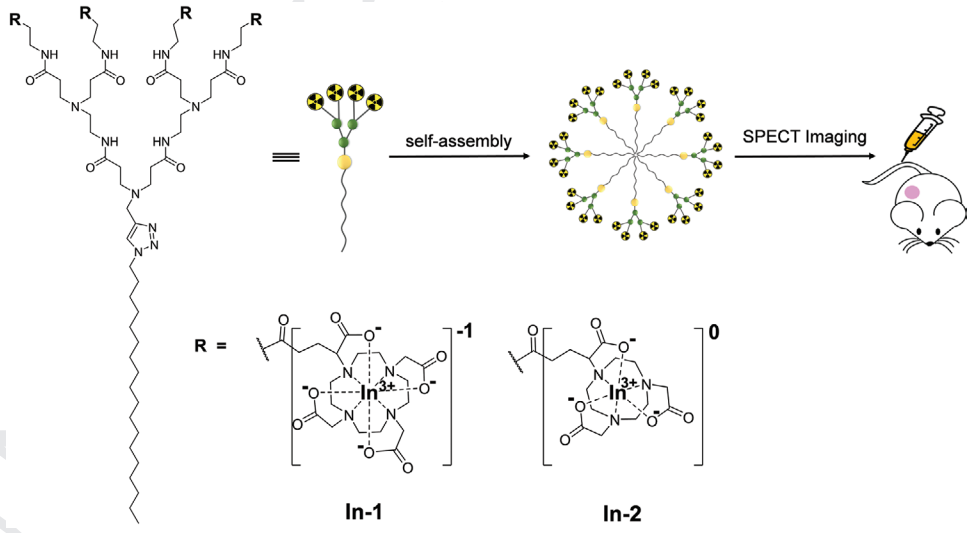

Figure 1. Schematic illustration of the supramolecular dendrimer nanosystems, based on the self-assembling amphiphilic dendrimers **In-1** and **In-2** bearing radionuclide In^{3+} terminals complexes with the macrocyclic DOTA and NOTA cages in the DOTAGA and NODAGA chelators, respectively, for single photon emission computed tomography (SPECT) imaging of tumors.

that positively charged nanoparticles preferentially accumulate in the liver,[3–5] our results clearly show that the presence of neutral surface regions of nanosystem with overall positively charged zeta potential could also result in drastically reduced liver uptake. Therefore, our findings provide new perspectives for improving the safety and biodistribution of various nanosystems for biomedical applications. Herein, we present and discuss our work in establishing **In-2** as a promising agent for SPECT imaging of tumors, highlighting the importance of surface charge for the biodistribution of nanoparticles as a general concept.

2. Results and Discussion

We prepared the dendrimer **2** bearing the macrocyclic NOTA cages at the terminals according to our previously reported synthesis.[13] However, in the present study, we reduced the quantity of the reagent NODA-GA(tBu)$_3$ by half in order to facilitate the purification procedures while maintaining the chemical integrity and high yield of product **2** (**Figure 2**A and Scheme S1, Supporting Information). Chelation of the stable isotope $^{115}In^{3+}$ by **2** was performed using $^{115}InCl_3$ at 25 °C for 10 min at pH 4.0–4.5 (Figure 2A). These conditions contrasted with those used for the synthesis of **In-1**, which required substantially higher temperatures (55 °C) and longer times (120 min). The successful complexation of four $^{115}In^{3+}$ ions by the macrocyclic NOTA scaffolds in **2** was confirmed using high-resolution mass spectroscopy, which revealed the isotopic pattern characteristic of the triply charged species [^{115}**In-2** + 3H]$^{3+}$ of the expected molecular structure (Figure 2C and Figure S1, Supporting Information).[23]

Previously, we also supported the synthesis of the dendrimer **In-1** carrying the DOTA cages through isothermal titration calorimetry (ITC).[14] We used the same approach to study the thermodynamics of the interaction between In^{3+} and the dendrimer **2** bearing the NOTA cages for generating **In-2** (Figure 2B). The titration of both dendrimers **1** and **2** with the

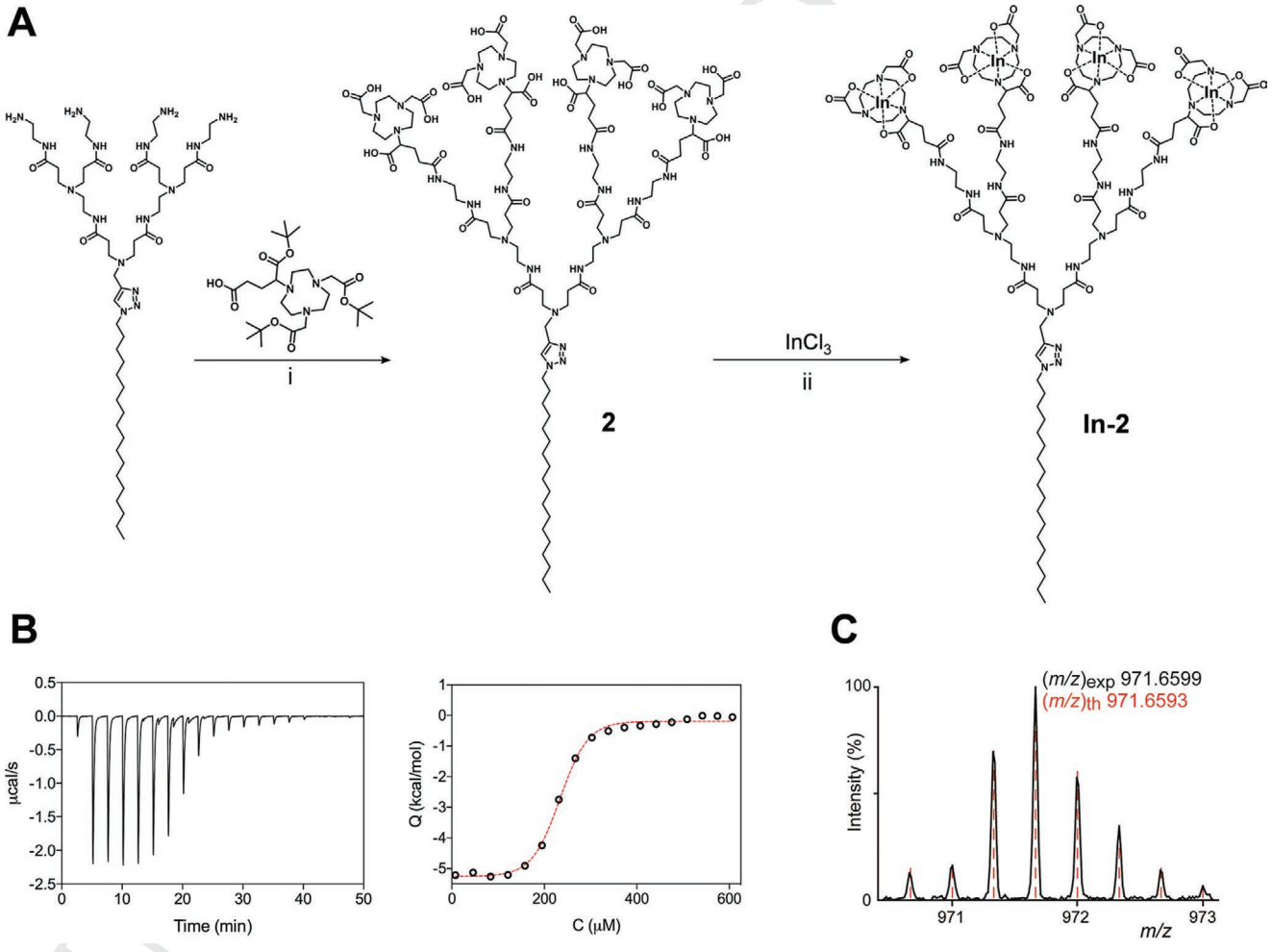

Figure 2. Synthesis of the amphiphilic dendrimer **2** and its chelation with the nonradioactive isotope [^{115}In]In^{3+} at the terminals. A) Synthesis scheme: (i) (a) NODA-GA(tBu)$_3$, PyBOP, NMM, DMF, 30 °C, 72 h; (b) TFA, CH_2Cl_2, 30 °C, 16 h. (ii) [^{115}In]$InCl_3$, 1.0 M HCl, 24 °C, 10 min. B) Isothermal titration calorimetry curve (right) for chelation of In^{3+} with the dendrimer **2**. The left panel shows measured heat power versus time elapsed during titration. C) High-resolution mass spectrum showing the isotopic pattern characteristic of the triply charged species [[^{115}In]**In-2** + 3H]$^{3+}$, which overlaps with the theoretical value presented with the red dashed line.

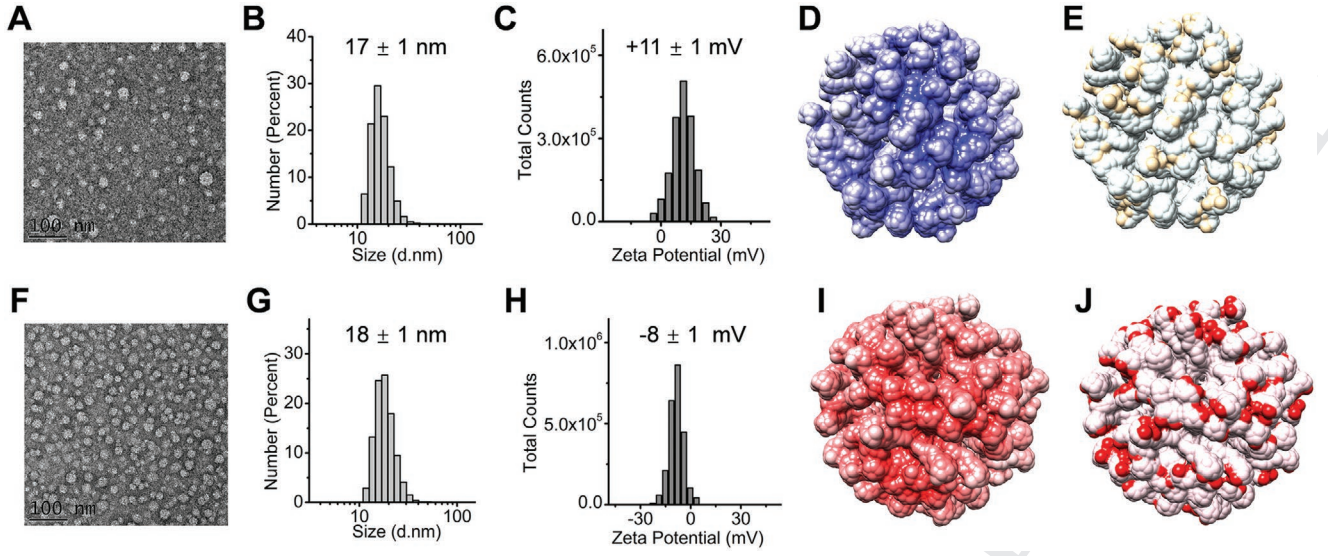

Figure 3. Comparison of the spontaneous self-assembling of the amphiphilic dendrimers **In-1** and **In-2** into small and uniform nanomicelles in water. A,F) Transmission electron microscopic imaging, B,G) dynamic light scattering analysis, C,H) surface zeta-potential measured using a zeta-nanosizer, D,I) electrostatic surface potential of the self-assembled nanostructures as extracted from the corresponding equilibrated molecular dynamics simulations, and E,J) representation of the surface charge distribution localized on the In^{3+}/NOTA complexes at the NODAGA terminals (neutral, ivory) and the In^{3+}/DOTA at the DOTAGA terminals (negative, red) for dendrimers **In-2** (upper row) and **In-1** (lower row). In panels (D) and (I), the red color represents a negatively charged surface, the dark blue color represents a positively charged surface, while the white color represents a neutral surface.

trivalent cation In^{3+} presented very similar calorimetric behaviors. The spontaneous formation of **In-2** was promoted by a favorable binding free energy (ΔG) of –7.64 kcal mol^{-1}. This value arises from the balanced and favorable contributions of both the entropic ($-T\Delta S$ = –2.21 kcal mol^{-1}) and the enthalpic (ΔH = –5.43 kcal mol^{-1}) components, which are similar to the binding thermodynamic parameters for **In-1** (ΔG = –7.86 kcal mol^{-1}, $-T\Delta S$ = –2.61, and ΔH = –5.25 kcal mol^{-1}). A 4:1 stoichiometry was also determined for the **In-2** complex by the ITC-derived number of occupied sites (n = 3.95), corroborating the results obtained using high-resolution mass spectroscopy (Figure 2C).

With the synthesized **In-2** in hand, we then examined the spontaneously self-assembling features of **In-2** in water. Using transmission electron microscopy, we observed the formation of small and spherical nanoparticles of an average size of 18 nm by **In-2** in water (**Figure 3**A), similar to those generated by the self-assembly of **In-1** (Figure 3F). Furthermore, dynamic light scattering analysis confirmed the presence of nanoparticles of similar sizes for both dendrimers **In-1** and **In-2** in water and in phosphate buffer at pH 7.4 (Figure 3B,G, and Figure S3, Supporting Information). This highlighted that, like **In-1**, **In-2** also self-assembled into nanomicelles. We then used a fluorescent spectroscopic assay with Nile Red to estimate the critical micelle concentration (CMC) of **In-2**, which was around 40 × 10^{-6} M, similar to the CMC value for **In-1** (49 × 10^{-6} M) (Figure S4, Supporting Information). In addition, we measured the surface zeta potential of the **In-2** nanomicelles, and obtained a positive value of +11 mV (Figure 3C), which could be ascribed to the interior tertiary amine functionality, since the In^{3+} complex with the NOTA ring in the NODAGA chelator at the dendrimer terminal is neutral. This is distinctly different from that of **In-1**, where each DOTA cage within the DOTAGA terminal in complex with In^{3+} has a net negative charge, thereby generating **In-1** nanomicelles with an overall negative zeta potential of –8 mV (Figure 3H).

To further confirm the spontaneous self-assembly of **In-1** and **In-2** into nanomicelles, we performed molecular dynamics simulations following a consolidated procedure.[13,14] Starting from randomly distributed monomers, we obtained stable spherical micelles for both systems during the timescale of the simulations (1.0 μs) (Figure 3D,F,I,J). The corresponding average micelle diameters computed from the equilibrated molecular

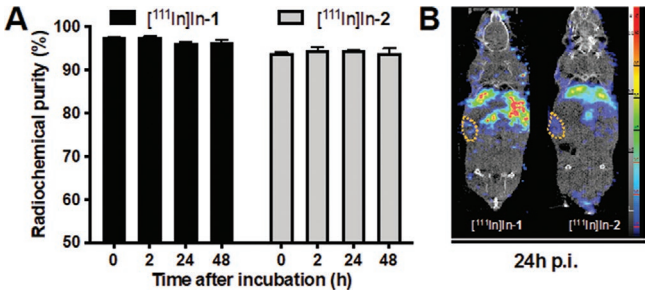

Figure 4. Radiolabeled dendrimers [^{111}In]**In-1** and [^{111}In]**In-2** for SPECT imaging in a mouse orthotopic xenograft model of pancreatic adenocarcinoma (SOJ-6 cell line) 24 h post-injection (p.i.). A) Radiochemical purity and stability of [^{111}In]**In-1** and [^{111}In]**In-2** assessed by instant thin layer chromatography immediately after incubation with human serum at 37 °C, and after 2, 24, and 48 h, respectively. Results show excellent radiochemical purities up to 48 h after radiosynthesis. B) Representative μSPECT/CT maximum intensity projection images of [^{111}In]**In-1** (left) and [^{111}In]**In-2** (right) 24 h after intravenous injection. The tumor is highlighted by orange dashed circles.

dynamics simulations were 15 and 13 nm for the **In-1** and **In-2** systems, respectively, which were in good agreement with the experimental results obtained using both dynamic light scattering and transmission electron microscopy. By inspecting the conformational structures of both micelles, no back-folding of the terminal groups was detected, in line with our previous findings obtained for similar systems.[13,14] Accordingly, the In^{3+}-bearing terminal units are all located at the periphery of the micelles in both the **In-1** and **In-2** systems. Further analysis of the electrostatic surface potential confirmed the foreseen effect of replacing the DOTA cage with the NOTA scaffold, with a negative electrostatic potential observed for **In-1** (Figure 3I) and a positive potential for **In-2** (Figure 3D), in agreement with the experimentally determined surface zeta potentials (Figure 3C,H). Moreover, the surface of the **In-1** micelle was characterized by the presence of localized negatively charged regions, corresponding to the trivalent In^{3+} ions in complex with the DOTA cages at the DOTAGA terminals (Figure 3J), while the **In-2** nanoparticles presented patches of neutral charge, corresponding to In^{3+} ions in complex with NOTA rings at the NODAGA terminals (Figure 3E).

Next, we prepared the radioactive dendrimer complex [^{111}In]**In-2** for SPECT imaging. Radiolabeling was performed using [^{111}In]In^{3+} in ammonium acetate buffer, and the obtained [^{111}In]**In-2** complex had an excellent radiochemical purity of over 93%, which was remarkably stable and maintained up for at least 48 h at 37 °C in human serum (**Figure 4**A). SPECT imaging using [^{111}In]**In-2** was first performed in orthotopically xenografted mice bearing human pancreatic adenocarcinoma SOJ-6 tumors, and the results obtained with [^{111}In]**In-1** were used as control for comparison. Co-registration with computed tomography (CT) enabled anatomical localization of the SPECT signals for further quantification. As seen in Figure 4B, a significantly improved image contrast for tumor visualization was obtained with [^{111}In]**In-2** compared to [^{111}In]**In-1**.

The improved tumor imaging achieved with [^{111}In]**In-2** compared to [^{111}In]**In-1** was further confirmed using a patient-derived xenograft model of pancreatic cancer (L-IPC cell line). As illustrated in **Figure 5**A,B,C, [^{111}In]**In-2** μSPECT signal quantification in the liver was significantly reduced compared to that of [^{111}In]**In-1** as soon as 2 h post-injection, and was maintained even 24 h and 48 h post-injection. Notably, the liver uptake was reduce by more than two times with [^{111}In]**In-2** compared with [^{111}In]**In-1**. Meanwhile, in the kidneys, [^{111}In]**In-2** μSPECT signal quantification was elevated up to 20% versus that of [^{111}In]**In-1**. Remarkably, the μSPECT signal of both [^{111}In]**In-1** and [^{111}In]**In-2** was drastically reduced in organs likely to generate background such as the heart, lungs, brain, muscle, and bladder at 24 and 48 h after administration, compared to quantifications performed 2 h post-injection, giving rise to better tumor imaging quality. When expressed as tumor-to-muscle or tumor-to-liver ratios, μSPECT/CT signal quantifications of tumor uptake of [^{111}In]**In-2** were significantly higher than those of [^{111}In]**In-1**, with up to a twofold increase (Figure 5D,E), translating into notably better tumor imaging quality.

In line with our original hypothesis, we tentatively rationalized the discrepancies in biodistribution to the difference in chelators and the resulting alteration in surface charge of **In-1** and **In-2**, since the size variation between the **In-1** and **In-2** nanomicelles was very small (Figure 3). As discussed above, after changing the DOTA cage in **In-1** to the NOTA scaffold in **In-2** at the dendrimer terminals, the zeta potential of the corresponding In^{3+}-labeled nanomicelles formed by these dendrimers changed accordingly (Figure 3E–J), leading to a more than twofold reduced accumulation of [^{111}In]**In-2** in the liver. Of note, the majority of published studies report that positively charged nanoparticles are more likely to accumulate in the liver than their negatively charged counterparts.[3–5] Our results, however, demonstrate that overall positively charged nanosystems exhibiting neutral regions on their surface can also exhibit reduced liver uptake. As a consequence, a significantly improved biodistribution and imaging profile was obtained with [^{111}In]**In-2** compared to [^{111}In]**In-1**. Our findings highlight that the impact on pharmacokinetics and biodistribution is dependent not only on the choice of chelator,[22,24] but also on the nature of the whole imaging probes. This overall feature may impact the ability of probes to bind to proteins in body fluids, depending on the different surface charges, and hence impacting the overall biodistribution.[25] In addition, lowering the liver uptake can also help to improve the safety and biodistribution profiles of the supramolecular nanosystems that have been developed for biomedical applications in general. Moreover, the dendrimer **In-2** enabled better tumor imaging, which was significantly enhanced (up to twofold) and long-lasting (up to 48 h after injection) for both tumor-to-muscle and tumor-to-liver ratios (Figure 5C,D). This feature is particularly interesting in developing imaging-guided internal radiotherapy.

It is noteworthy that the mice receiving the radioactive [^{111}In]**In-2** did not display any abnormal behaviors or adverse effects during all experimental imaging procedures. Furthermore, healthy mice that received the nonradioactive **In-2** did not exhibit any organ damage or blood biochemistry defects, even when the administered dose of **In-2** was 10 times higher than that required for SPECT imaging (**Figure 6**). As shown in Figure 6A, histological analysis of organs from mice treated with **In-2** revealed no gross lesions or significant underlying pathologies in any organ tissue sections. Also, several major blood biochemistry parameters including alanine transaminase, aspartate transaminase, total bilirubin, creatinine, urea, total protein, alkaline phosphatase, triacylglycerol, and total cholesterol remained at the levels comparable to those found in untreated mice (Figure 6B). This highlighted that no acute events were associated with **In-2** in terms of normal liver, kidney, and muscle function, further confirming that the main organs functioned well after treatment with **In-2**. All these data demonstrate that [^{111}In]**In-2** produces no adverse effects, but delivers effective SPECT imaging quality.

3. Conclusion

By replacing the DOTA cage with the NOTA scaffold to chelate the radionuclide In^{3+}, we established a new amphiphilic dendrimer **In-2** bearing neutral coordination complexes

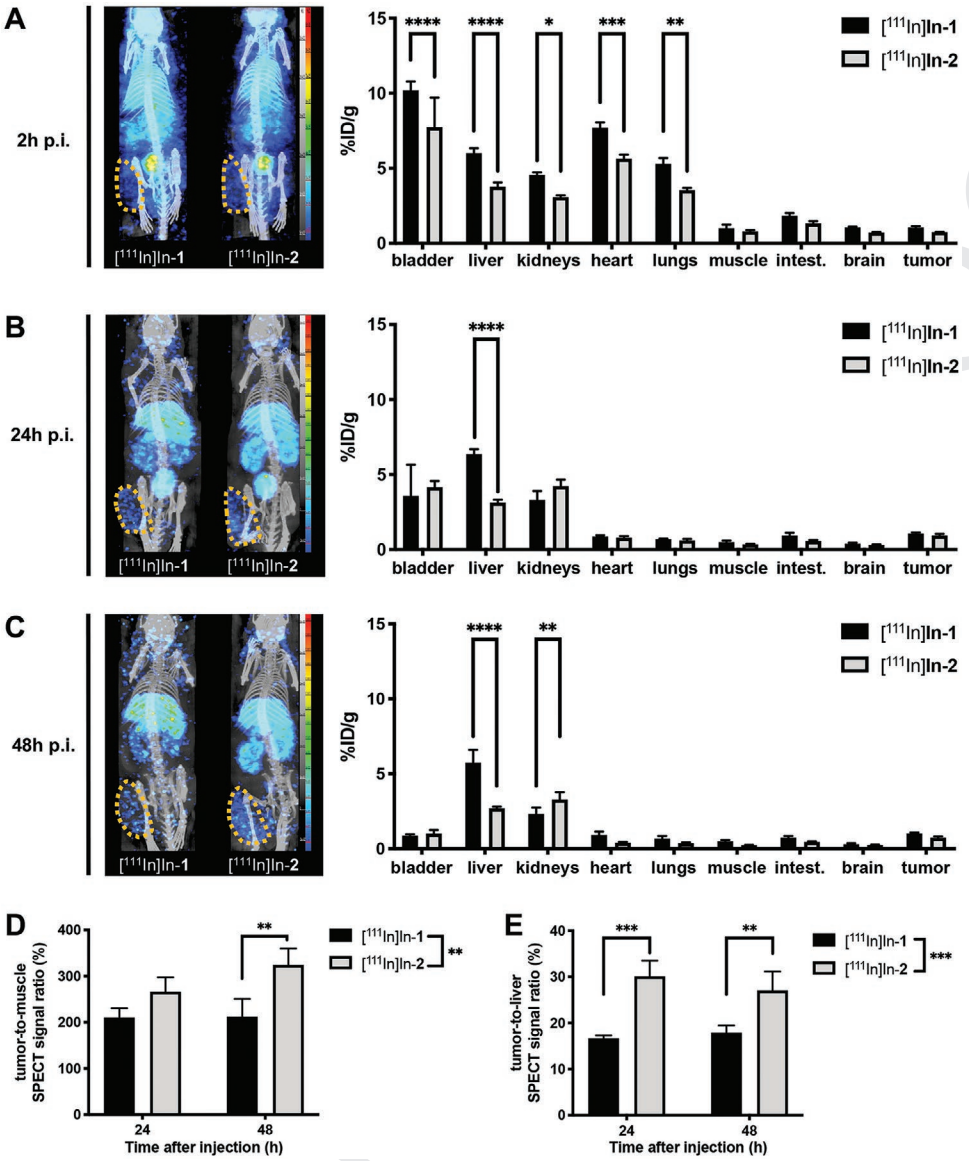

Figure 5. Radiolabeled dendrimer [^{111}In]**In-1** and [^{111}In]**In-2** for SPECT imaging in a patient-derived subcutaneous xenograft model of pancreatic cancer (L-IPC). A–C) Representative µSPECT/CT maximum intensity projection images of [^{111}In]**In-1** and [^{111}In]**In-2** 2 h ((A), left), 24 h ((B), left), and 48 h ((C), left) after intravenous injection. The tumor is highlighted in orange dashed circles. Biodistributions of [^{111}In]**In-1** and [^{111}In]**In-2** were quantified in each organ by µSPECT/CT 2 h ((A), right), 24 h ((B), right) and 48 h ((C), right) post-injection (p.i.). Data are expressed as the mean percentage of whole-body activity per gram of tissue at the time of acquisition ($n = 3$ mice). The two nanosystems showed significantly different signal quantifications 2 h p.i. in the bladder (****$p < 0.0001$), liver (****$p < 0.0001$), kidneys (*$p = 0.0118$), heart (***$p = 0.0002$), and lungs (**$p = 0.0024$), 24 h p.i. in the liver (****$p < 0.0001$), and 48 h p.i. in the liver (****$p < 0.0001$) and kidneys (**$p < 0.0014$), comparing [^{111}In]**In-2** with [^{111}In]**In-1** (2-way ANOVA followed by a Sidak's post-hoc test). D) Tumor-to-muscle ratio µSPECT/CT signal quantifications of tumor uptake of [^{111}In]**In-2** were significantly higher than those of [^{111}In]**In-1** 48 h p.i. (**$p = 0.0052$) and most interestingly over time (**$p = 0.0018$, two-way ANOVA followed by a Sidak's post-hoc test). E) Tumor-to-liver ratios µSPECT/CT signal quantifications of tumor uptake of [^{111}In]**In-2** were significantly higher than those of [^{111}In]**In-1** 24 h p.i. (***$p < 0.0007$), 48 h p.i. (**$p = 0.0075$) and most interestingly over time (***$p = 0.0001$, two-way ANOVA followed by a Sidak's post-hoc test).

with the trivalent In^{3+} ions at the dendrimer terminals for SPECT imaging. This modification had a drastic impact, generating significantly improved tumor imaging and a beneficial biodistribution profile. Notably, the uptake of **In-2** in the liver was reduced significantly, by more than twofold compared with that of **In-1**; at the same time, the imaging contrast was also considerably enhanced up to twofold and sustained even up to 48 h after injection. This study presents not only the supramolecular dendrimer nanosystem **In-2** for safe and effective SPECT imaging of tumors, but also new perspectives for improving the safety and biodistribution of supramolecular nanosystems for biomedical applications, such as theranostics based on imaging-guided internal radiotherapy.

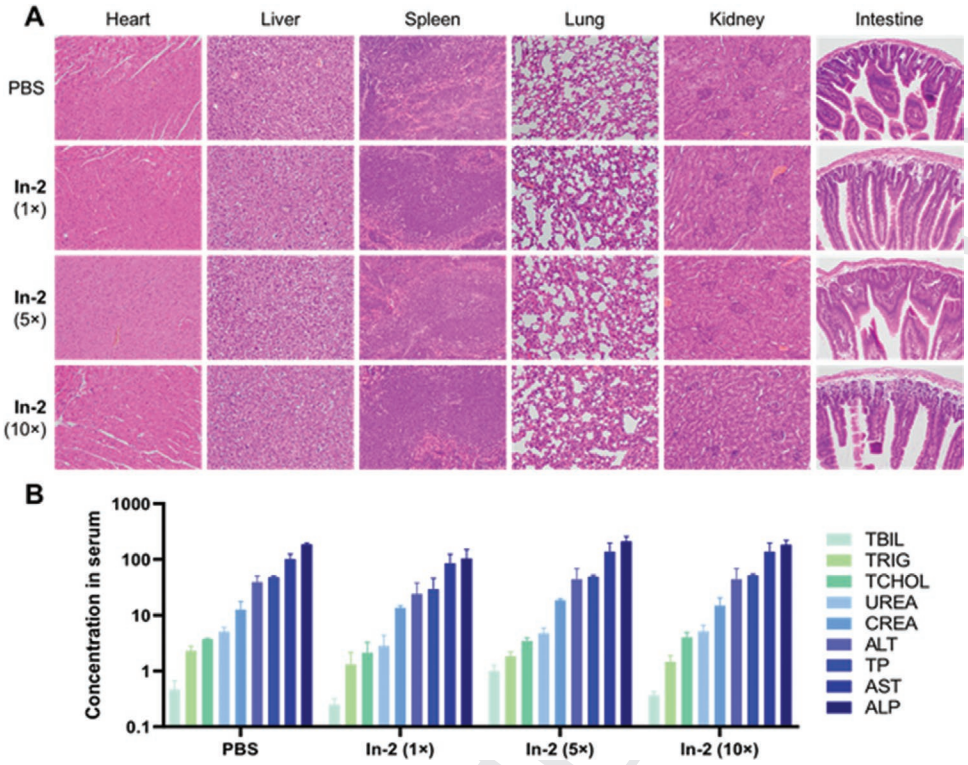

Figure 6. In vivo toxicity assessment of **In-2** in healthy mice at different doses. 1×, 5×, and 10× indicate that the formulations were administered at a dose equal to the SPECT-imaging dose, 5 times the imaging dose, and 10 times the imaging dose, respectively. A) Histopathological analysis of the major organs from mice treated with **In-2**. Tissue samples were collected 24 h post-administration. No significant histopathological changes were observed in any of the tissue sections. Images were enlarged 200 times with the microscope. B) Major serum biochemistry parameters measured in mouse serum collected at 24 h post-injection. Alanine transaminase (ALT), aspartate transaminase (AST), and alkaline phosphatase (ALP) were measured in U L^{-1}; urea, triacylglycerol (TRIG), and total cholesterol (TCHOL) were measured in mmol L^{-1}; creatinine (CREA) and total bilirubin (TBIL) were measured in µmol L^{-1}; total protein (TP) was measured in g L^{-1}. Data are shown as mean ± SD.

Supporting Information

Supporting Information is available from the Wiley Online Library or from the author.

Acknowledgements

The authors thank Michel Skandalovski (CERIMED, Aix-Marseille University), Samy Vigier, and Sandrine Pons (Faculty of Pharmacy, Aix-Marseille University) for technical support. This work was supported by the Ligue Nationale Contre le Cancer (L.P., Z.L.), China Scholarship Council (L.D.), Italian Association for Cancer Research (IG17413) (S.P.), the French National Research Agency under the frame of the Era-Net EURONANOMED European Research projects "NANOGLIO", "TARBRAINFECT", and "NAN-4-TUM" (L.P.), H2020 NMBP "SAFE-N-MEDTECH" (L.P.), the National Natural Science Foundation of China (31871003, 31901053) (Y.H.), and Ecole Doctorale 62 Sciences de la vie et de la santé, Aix-Marseille Université (B.L.). This article is based upon work from COST Action CA 17140 "Cancer Nanomedicine from the Bench to the Bedside" supported by COST (European Cooperation in Science and Technology).

Conflict of Interest

The authors declare no conflict of interest.

Author Contribution

L.D., Z.L., and B.L. contributed equally to this work. L.P. coordinated the project. L.D., Z.L., A.B., and P.G. synthesized the agents. L.D., Z.L., A.T., S.G., A.B., and P.G. made the characterization of the agents. E.L., D.M., and S.P. provided ITC and molecular modeling data. E.M. and P.G. prepared the SOJ-6 animal model. L.D., Y.J., and J.L. prepared the LIPC animal model. P.G., B.L., L.B., and S.F. performed imaging experiments. M.Z., W.S., and Y.H. performed toxicity study. L.D., Z.L., A.T., P.G., B.L., A.B., B.G., Y.H., E.L., S.P., and L.P. analyzed data. L.P. wrote the paper with contribution from L.D., Z.L., A.T., E.L., S.P., P.G., B.G., and Y.H. All authors proofed the manuscript.

Keywords

dendrimer, metal chelators, self-assembling, SPECT imaging, supramolecular nanosystems, surface charge

Received: May 27, 2020
Revised: June 29, 2020
Published online:

[1] M. L. James, S. S. Gambhir, *Physiol. Rev.* **2012**, *92*, 897.
[2] C. Li, *Nat. Mater.* **2014**, *13*, 110.

[3] H. Chen, W. Zhang, G. Zhu, J. Xie, X. Chen, *Nat. Rev. Mater.* **2017**, *2*, 17024.
[4] E. K.-H. Chow, D. Ho, *Sci. Transl. Med.* **2013**, *5*, 216rv214.
[5] E.-K. Lim, T. Kim, S. Paik, S. Haam, Y.-M. Huh, K. Lee, *Chem. Rev.* **2015**, *115*, 327.
[6] H. Maeda, J. Wu, T. Sawa, Y. Matsumura, K. Hori, *J. Controlled Release* **2000**, *65*, 271.
[7] M. A. Mintzer, M. W. Grinstaff, *Chem. Soc. Rev.* **2011**, *40*, 173.
[8] A. R. Menjoge, R. M. Kannan, D. A. Tomalia, *Drug Discovery Today* **2010**, *15*, 171.
[9] D. Ling, L. Zhenbin, D. Dinesh, K. Chai-Lin, B. Monique, P. Ling, *Sci. China Mater.* **2018**, *61*, 1420.
[10] Z. Qiao, X. Shi, *Prog. Polym. Sci.* **2015**, *44*, 1.
[11] L. Zhao, X. Shi, J. Zhao, *Drug Delivery.* **2017**, *24*, 81.
[12] L. Zhao, X. Shi, J. Zhao, in *Nanotechnology Characterization Tools for Biosensing and Medical Diagnosis* (Eds: C. Kumar), Springer, Berlin, Heidelberg **2018**, p. 509.
[13] P. Garrigue, J. Tang, L. Ding, A. Bouhlel, A. Tintaru, E. Laurini, Y. Huang, Z. Lyu, M. Zhang, S. Fernandez, L. Balasse, W. Lan, E. Mas, D. Marson, Y. Weng, X. Liu, S. Giorgio, J. Iovanna, S. Pricl, B. Guillet, L. Peng, *Proc. Natl. Acad. Sci. U. S. A.* **2018**, *115*, 11454.
[14] L. Ding, Z. Lyu, A. Tintaru, E. Laurini, D. Marson, B. Louis, A. Bouhlel, L. Balasse, S. Fernandez, P. Garrigue, E. Mas, S. Giorgio, S. Pricl, B. Guillet, L. Peng, *Chem. Commun.* **2020**, *56*, 301.
[15] D. Ni, E. B. Ehlerding, W. Cai, *Angew. Chem., Int. Ed.* **2019**, *58*, 2570.
[16] T. J. Wadas, E. H. Wong, G. R. Weisman, C. J. Anderson, *Chem. Rev.* **2010**, *110*, 2858.
[17] O. Israel, O. Pellet, L. Biassoni, D. De Palma, E. Estrada-Lobato, G. Gnanasegaran, T. Kuwert, C. la Fougère, G. Mariani, S. Massalha, D. Paez, F. Giammarile, *Eur. J. Nucl. Med. Mol. Imaging* **2019**, *46*, 1990.
[18] R. van der Meel, E. Sulheim, Y. Shi, F. Kiessling, W. J. M. Mulder, T. Lammers, *Nat. Nanotechnol.* **2019**, *14*, 1007.
[19] Y. Tsvetkova, N. Beztsinna, M. Baues, D. Klein, A. Rix, S. K. Golombek, W. Al Rawashdeh, F. Gremse, M. Barz, K. Koynov, S. Banala, W. Lederle, T. Lammers, F. Kiessling, *Nano Lett.* **2017**, *17*, 4665.
[20] B. Mitran, Z. Varasteh, R. K. Selvaraju, G. Lindeberg, J. Sörensen, M. Larhed, V. Tolmachev, U. Rosenström, A. Orlova, *Int. J. Oncol.* **2016**, *48*, 2124.
[21] T. I. Kostelnik, C. Orvig, *Chem. Rev.* **2019**, *119*, 902.
[22] E. W. Price, C. Orvig, *Chem. Soc. Rev.* **2014**, *43*, 260.
[23] C. Brevard, P. Granger, in *Handbook of High Resolution Multinuclear NMR* (Eds: C. Brevard, P. Granger), John Wiley and Sons, Inc., xxxx **1981**.
[24] J. Strand, H. Honarvar, A. Perols, A. Orlova, R. K. Selvaraju, A. E. Karlström, V. Tolmachev, *PLoS One* **2013**, *8*, 70028.
[25] S. Lamichhane, S. Lee, *Arch. Pharmacal Res.* **2020**, *43*, 118.

NANO MICRO small

Please complete this form and return it via E-Mail to the Editorial Office:
small@wiley-vch.de

Reprint Order Form

Manuscript No.: _____

Customer No.: (if available) _____

Purchase Order No.: _____

Author: _____

Charges for Reprints in Euro (excl. VAT), prices are subject to change. Minimum order 50 copies.

No. of pages	50 copies	100 copies	150 copies	200 copies	300 copies	500 copies
1– 4	345,—	395,—	425,—	445,—	548,—	752,—
5– 8	490,—	573,—	608,—	636,—	784,—	1077,—
9–12	640,—	739,—	786,—	824,—	1016,—	1396,—
13–16	780,—	900,—	958,—	1004,—	1237,—	1701,—
17–20	930,—	1070,—	1138,—	1196,—	1489,—	2022,—
every additional 4 pages	147,—	169,—	175,—	188,—	231,—	315,—

Information regarding VAT: The charges for publication of *reprints/poster* are considered to be "supply of services" and therefore subject to German VAT. However, if you are an institutional customer outside Germany, the tax can be waived if you provide us with the valid VAT number of your company. Non-EU customers may have a VAT number starting with "EU" instead of their country code, if they are registered with the EU tax authorities. If you do not have a valid EU VAT number and you are a taxable person doing business in a non-EU country, please provide a certification from your local tax authorities confirming that you are a taxable person under local tax law. Please note that the certification must confirm that you are a taxable person and are conducting an economic activity in your country. **Note:** certifications confirming that you are a tax-exempt legal body (non-profit organization, public body, school, political party, etc.) in your country do not exempt you from paying German VAT.

Please send me send bill me for

☐ no. of reprints

☐ high-resolution PDF file (330 Euro excl. VAT)
E-mail address: _____

❖ Special Offer:
If you order 200 or more reprints you will get a PDF file for half price.

Please note: It is not permitted to present the PDF file on the internet or on company homepages.

Cover Posters (prices excl. VAT)
Posters of published covers are available in two sizes:

☐ DIN A2 42 x 60 cm / 17 x 24in (one copy: 39 Euro)

☐ DIN A1 60 x 84 cm / 24 x 33in (one copy: 49 Euro)

Postage for shipping (prices excl. VAT)
overseas +25 Euro
within Europe +15 Euro

_____
Date, Signature

VAT number: _____

Mail reprints / copies of the issue to:

_____
_____
_____
_____
_____

Send bill to:

_____
_____
_____
_____

☐ **I will pay by bank transfer**

☐ **I will pay by credit card**

VISA, Mastercard and AMERICAN EXPRESS

For your security please use this link (Credit Card Token Generator) to create a secure code Credit Card Token and include this number in the form instead of the credit card data. Click here:
https://www.wiley-vch.de/editorial_production/index.php

CREDIT CARD TOKEN NUMBER

						V									

Wiley-VCH Verlag GmbH & Co. KGaA – A company of John Wiley & Sons, Inc. -
Location of the Company: Weinheim - Trade Register: Mannheim, HRB 432833.
Chairman of the Supervisory Board: John Kritzmacher
General Partner: John Wiley & Sons GmbH, Location: Weinheim –
Trade Register Mannheim, HRB 432296 – Managing Director: Sabine Haag and Dr. Guido Herrmann

WILEY-VCH